ACS APPLIED MATERIALS & INTERFACES

Research Article

www.acsami.org

Designing Heterogeneous Chemical Composition on Hierarchical Structured Copper Substrates for the Fabrication of Superhydrophobic Surfaces with Controlled Adhesion

Zhongjun Cheng,[†] Rui Hou,[†] Ying Du,[†] Hua Lai,[†] Kewei Fu,[†] Naiqing Zhang,[†,‡] and Kening Sun*[,†,‡]

[‡]State Key Laboratory of Urban Water Resource and Environment, School of Municipal and Environmental Engineering, [†]Natural Science Research Center, Academy of Fundamental and Interdisciplinary Sciences, Harbin Institute of Technology, Harbin, Heilongjiang 150090, P. R. China

Supporting Information

ABSTRACT: Controlling water adhesion is important for superhydrophobic surfaces in many applications. Compared with numerous researches about the effect of microstructures on the surface adhesion, research relating to the influence of surface chemical composition on the surface adhesion is extremely rare. Herein, a new strategy for preparation of tunable adhesive superhydrophobic surfaces through designing heterogeneous chemical composition (hydrophobic/hydrophilic) on the rough substrate is reported, and the influence of surface chemical composition on the surface adhesion are examined. The surfaces were prepared through self-assembling of mixed thiol (containing both $HS(CH_2)_9CH_3$ and $HS(CH_2)_{11}OH$) on the hierarchical structured copper substrates. By simply controlling the concentration of $HS(CH_2)_{11}OH$ in the modified solution, tunable adhesive superhydrophobic surfaces can be obtained. The adhesive force of the surfaces can be increased from extreme low (about 8 μN) to very high (about 65 μN). The following two reasons can be used to explain the tunable effect: one is the number of hydrogen bond for the variation of surface chemical composition; and the other is the variation of contact area between the water droplet and surface because of the capillary effect that results from the combined effect of hydrophilic hydroxyl groups and microstructures on the surface. Noticeably, water droplets with different pH (2−12) have similar contact angles and adhesive forces on the surfaces, indicating that these surfaces are chemical resistant to acid and alkali. Moreover, the as-prepared surfaces were also used as the reaction substrates and applied in the droplet-based microreactor for the detection of vitamin C. This report provides a new method for preparation of superhydrophobic surfaces with tunable adhesion, which could not only help us further understand the principle for the fabrication of tunable adhesive superhydrophobic surfaces, but also potentially be used in many important applications, such as microfluidic devices and chemical microreactors.

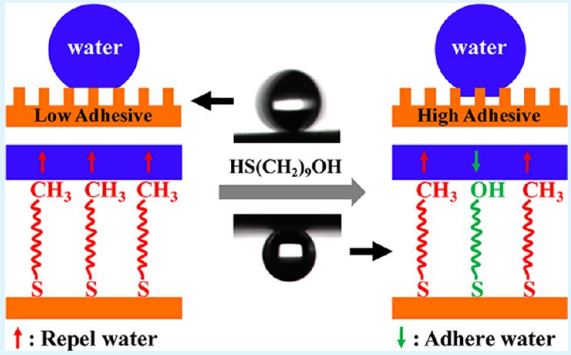

KEYWORDS: *superhydrophobic surfaces, tunable adhesion, heterogeneous chemistry, microdroplet transportation*

INTRODUCTION

In the past few years, superhydrophobic surface becomes a new research focus for the wide applications,[1] for example: self-cleaning,[2−9] oil/water separation,[10−13] antireflection,[14] anti-bioadhesion,[15] fluidic drag reduction,[16] and transportation of microdroplet.[17,18] Different applications need the surfaces with different adhesions because it is the adhesive property that ultimately determines the dynamic action of the liquid on the surface.[19] According to different mobility of water droplet on the surfaces, superhydrophobic surfaces can generally be divided into two kinds: one kind is superhydrophobic low-adhesion surface,[20−24] and the other kind is superhydrophobic high-adhesion surface.[25−28] Through numerous researches, people find that different adhesions on these surface are ascribed to different morphologies and microstructures that would result in different wetting states for droplets on the surfaces.[26,29,30] Taking the inspiration of these findings, dramatic efforts have been expended on design and fabrication of rough substrates with controlled microstructures to realize the tunable adhesion for water droplets.[31−61] For instance, construction the PDMS arrays with microbowls and microlens structures through lithography;[32] preparation of porous TiO_2 nanostructured films with controlled pore sizes through electrodeposition process;[34] and construction of MnO_2 surfaces with nanorod, cactus, and meshlike structures through hydrothermal process.[35]

In addition to microstructures, another factor, surface chemical composition is also crucial in controlling the surface adhesion. It is reasonable to expect that tunable adhesive superhydrophobic surfaces can be prepared through controlling

Received: June 30, 2013
Accepted: August 7, 2013
Published: August 7, 2013

   dx.doi.org/10.1021/am4025577 | ACS Appl. Mater. Interfaces 2013, 5, 8753−8760

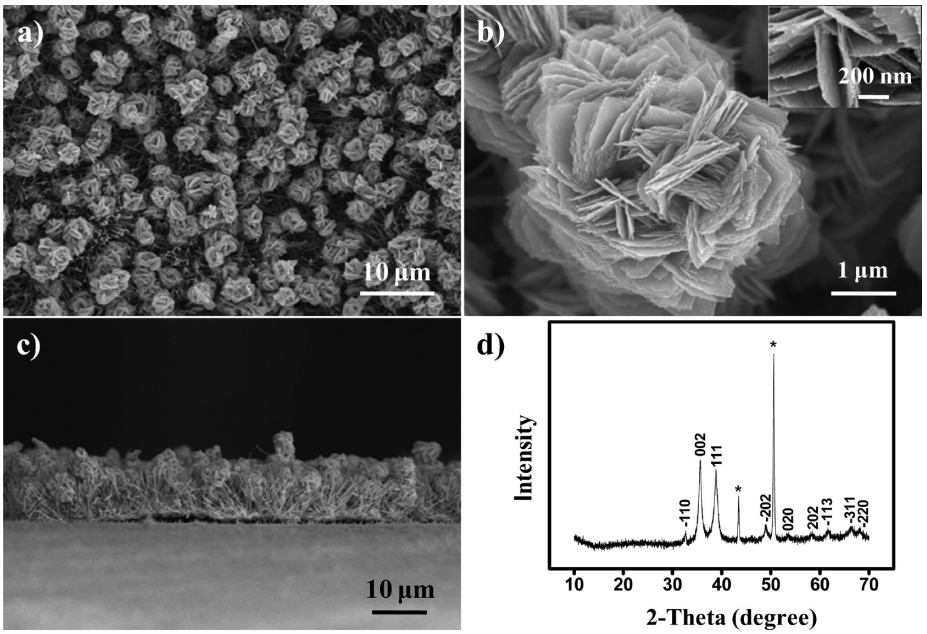

Figure 1. (a, b) SEM images of the copper substrate with low and high magnifications, respectively. Inset in b is the magnified image of one microsphere. (c) Cross-sectional view of the hierarchical CuO on the substrate. (d) XRD pattern of the as-prepared surface.

the surface chemical composition. In fact, such research is very important because it can not only give us some new ideas to design and fabricate novel tunable adhesive superhydrophobic surfaces, but also help us further understand the principle for fabrication such superhydrophobic surface. However, so far, correlative research is still rare.[62−65]

Herein, using the self-assemble monolayer technique, we prepared superhydrophobic surfaces with controlled surface chemical compositions, and investigated the effect of surface chemical composition on the water adhesion. In detail, the hierarchical CuO was prepared first on copper foils and used as substrates, then these substrates were modified with mixed thiols (containing both $HS(CH_2)_{11}OH$ and $HS(CH_2)_9CH_3$) to endow the substrates with heterogeneous chemical composition (hydrophobic/hydrophilic). By simply controlling the concentration of $HS(CH_2)_{11}OH$ in the modified solution, tunable adhesive superhydrophobic surfaces can be obtained, and the adhesive force can be controlled from extreme low (about 8 μN) to very high (about 65 μN). In addition, the obtained surfaces are chemically stable to acidic and basic water droplets. These special abilities allows us demonstrate an application of the surfaces in the droplet-based microreactor.

EXPERIMENTAL SECTION

Materials. $HS(CH_2)_9CH_3$, $HS(CH_2)_{11}OH$, trichloro(propyl)silane (Aldrich, Germany), $(NH_4)_2S_2O_8$, 2, 6-Dichloroindophenol sodium salt, Copper foils (99.9%), NaOH, vitamin C, and ethanol were purchased from Beijing Fine Chemical Co., China. Ultrapure water are obtained from Milli-Q system (>1.82 MΩ cm).

Preparation of the Hierarchical Structured CuO on the Copper Substrates. The process for the preparation of hierarchical structured CuO on the copper substrate is similar as reported.[66,67] Briefly, copper substrates were first sequentially cleaned with acetone, ethanol, and ultrapure water, and then immersed into a solution containing both NaOH (2.5 M) and $(NH_4)_2S_2O_8$ (0.1 M) for about 1 h. After that, these copper substrates were taken out, rinsed with abundant ultrapure water and dried with N_2. At last, these copper substrates were heated at 120 °C for 1 h to complete dehydration and followed by annealing at 180 °C for 2 h to form the CuO.

Modification the Hierarchical Structured Copper Substrates with Thiol Molecules. The copper substrates with hierarchical sturcured CuO were first covered with a Au layer in a sputter coater (Leica EM, SCD500), after that, these copper substrates were put into the thiols solution containing the $HS(CH_2)_9CH_3$ and $HS(CH_2)_{11}OH$ for about 12 h. The mole fraction of $HS(CH_2)_{11}OH$ in the solution was changed from o to 1 and the whole concentration of the mixed thiol in ethanol solution is fixed at 1 mmol L^{-1}. At last, these substrates were taken out, rinsed with abundant ethanol, and dried with N_2.

Silanization Procedure. The surface prepared with X_{OH} = 0.3 (X_{OH} is the mole fraction of the $HS(CH_2)_{11}OH$ in the modified solution) was placed in a vacuum desiccators with a beaker containing 0.2 mL liquid trichloro(propyl)silane. A vacuum pump was used to decrease the vacuum degree of the desiccator to about 5000 Pa and this condition was kept for about 12 h. The trichloro(propyl)silane would vaporize and react with the hydroxyl groups on surface. Then, the substrates were washed with abundant ethanol and further dried with N_2.

Instrumentation and Characterization. The morphology of the copper surface were observed using a field-emission scanning electron microscope (HITACHI, SU8010). The contact angles, sliding angles, advancing contact angles and receding contact angles were examined on the JC 2000D5 (provied by Shanghai Zhongchen Digital Technology Apparatus Co., Ltd.) at ambient temperature, the volume of the test droplet is about 4 μL. The average values of contact angles were attained by examing five different positions on one surface. During the investigation of sliding angles, a 4 μL droplet was first placed on the surface, and then the surface was tilted until the droplet began to slide. The advancing contact angles and the receding contact angles were acquired through increasing and decreasing the water volume on the surface, respectively. The water with different pH was obtained through adding hydrochloric acid and sodium hydroxide, and the pH values were measured by a pH meter (PB-10, Sartorius). The adhesive force of the surface was measured through a high-sensitivity microelectromechanical balance (Dataphysics DCAT 11, Germany); meanwhile, the process was recorded with an charge coupled device (CCD) camera. A water droplet (4 μL) was first hung on a metal ring, which has been fixed to the balance. The stage with the surface was moved upward at a speed of 0.02 mm s^{-1}, after contact with the droplet, it started to move down. The maximum force recorded when the droplet is just leaving the surface is defined as the adhesive force. X-ray diffraction (XRD) was examined using a X-ray diffractometer

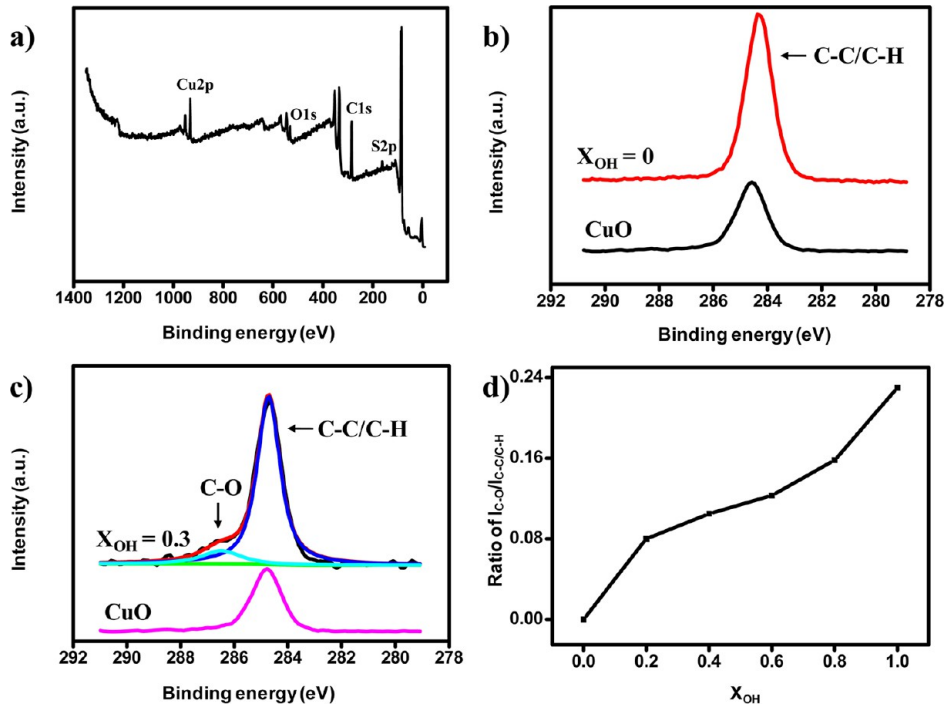

Figure 2. (a) XPS survey spectrum of the surface prepared with X_{OH} = 0.3 (X_{OH} means the mole fraction of $HS(CH_2)_{11}OH$ in modified solution). (b) High-solution C 1s XPS spectra of the initial CuO surface and the surface modified with $HS(CH_2)_9CH_3$. (c) High-solution C 1s XPS spectra of the initial CuO surface and the surface prepared with X_{OH} = 0.3. (d) Dependence of the ratio of $I_{C-O}/I_{C-C/C-H}$ on the X_{OH}.

(X'Pert Pro MPD, Philips, Netherlands) with Cu Ka radiation (λ = 0.15405 nm), the test range of 2θ is from 10 to 70°. X-ray photoelectron spectroscopy (XPS) data were attained with a K-Alpha electron spectrometer using Al Ka (1486.6 eV) radiation (Thermo Fisher Scientific Company). The deconvolution of the C1s was conducted by means of XPS Peak processing software version 4.1. The IR spectrum was obtained on the PerkinElmer Spectrum 100 FT-IR Spectrometer.

RESULTS AND DISCUSSION

To obtain the superhydrophobic surfaces, a proper rough structure is necessary.[23] In this work, copper was chosen as the substrate for its wide application in our daily life. The hierarchical CuO on the copper substrate was fabricated by a simple solution immersion process (more details see Supporting Information Figure S1–S2).[66,67] Briefly, a clean copper foil was put into an aqueous solution containing NaOH and $(NH_4)_2S_2O_8$ for about 1 h and further dried in an oven at 180 °C for about 2 h, then black CuO can be obtained on the copper substrate according to the following equations:

$$Cu + NaOH + (NH_4)_2S_2O_8 \rightarrow Cu(OH)_2 + Na_2SO_4 + NH_4 + H_2O \quad (1)$$

$$Cu(OH)_2 \xrightarrow{\Delta} CuO + H_2O \quad (2)$$

The morphology of the surface was investigated with a scanning electron microscopy (SEM). From Figure 1a, one can observe that the flower-like microspheres with diameters ranging from 3 to 5 μm standing on the nanowires arrays. Through the amplified image (Figure 1b), it can be found that the microsphere is composed of nanoslices, and the thickness of one slice is about 35 nm (inset in Figure 1b). Furthermore, one can also find that the nanowires under the microsphere are 50–250 nm in diameter (see the Supporting Information, Figure S3) and the total thickness of the film is about 15 μm (Figure 1c). As is known, surface with such hierarchical structures can enhance the surface hydrophobicity to the superhydrophobicity.[3−6] The crystal structure of our surface was analyzed by the X-ray diffraction (XRD). The result is in accordance with above equations, and the obtained hierarchical structures are CuO. As shown in Figure 1d, except those marked with stars that can be ascribed to the copper substrate, all the indexed diffraction peaks can be assigned to the monoclinic phase of CuO.[67]

To achieve the heterogeneous chemical composition on the rough substrate, two different thiol molecules ($HS(CH_2)_{11}OH$ and $HS(CH_2)_9CH_3$) were chosen for the modification of the substrates.[68−70] Figure 2a shows the X-ray photoelectron spectroscopy (XPS) survey spectrum of the surface prepared with X_{OH} = 0.3 (X_{OH} is the mole fraction of $HS(CH_2)_{11}OH$ in modified solution), one can observe the element Cu, O, C, and S on the surface. From the high-resolution XPS spectra for C 1s, more information about the variation of surface composition can be observed. On the surface modified with single hydrophobic $HS(CH_2)_9CH_3$ (X_{OH} = 0, Figure 2b), the intensity of C 1s peak at 284.8 eV ascribed to C−C/C−H is increased apparently compared with that of the as-prepared CuO surface (a weak peak can be found in the C 1s spectrum of CuO film is ascribed to little impurity). When the X_{OH} is increased, for example X_{OH} = 0.3 (Figure 2c), in addition to the increased intensity, a new peak at 286.6 eV arises and can be ascribed to C−O,[66] indicating that the molecule $HS(CH_2)_{11}OH$ has been assembled on the surface successfully. Noticeably, one can also find that with increasing the X_{OH} in the modified solution, the C1s peak intensity of C−O comparing with that of the C−C/C−H is increased (Figure 2d), indicating that the amount of surface hydroxyl groups can be increased as the X_{OH} is increased. From the above, it is reasonable to conclude that through the self-assemble process, we can control the surface

composition by changing the composition of the mixed solution.

The wetting performances of as-prepared surfaces were investigated by the contact angle measurements. Before modification, the CuO substrate is superhydrophilic, and the contact angle is about 0° (see the Supporting Information, Figure S4), however, after the modification, the phenomenon would be different. From Figure 3a, it can be seen that the surface can change from superhydrophobicity to superhydrophilicity, and the contact angles decrease from about 158 to 0° as the X_{OH} is increased. As is known, the surface wettability is controlled by both the microstructures and the surface chemical compositions.[71] In this work, all the copper substrates have the similar geometrical microstructures and the chemical composition is the main factor that influences the wettability. As the X_{OH} is increased, more hydrophilic hydroxyl groups would be assembled on the copper substrate, together with the enhanced effect of the hierarchical structures,[72,73] the contact angles on the surfaces would decrease from very high (larger than 150°) to extremely low (about 0°).

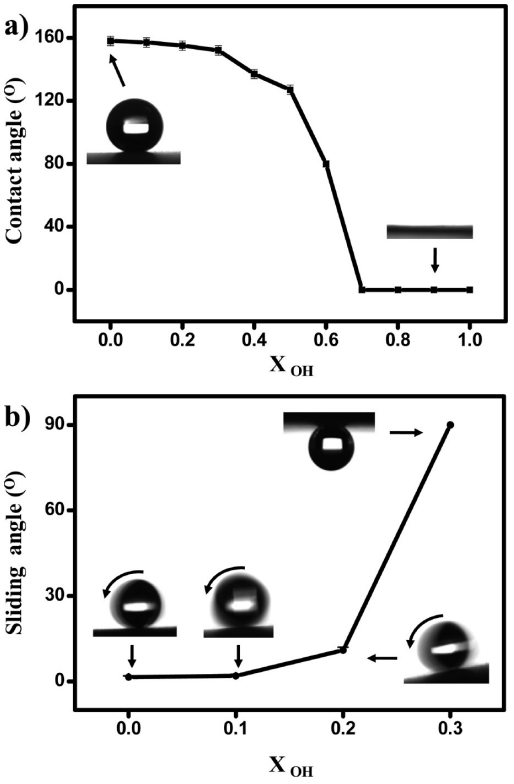

Figure 3. Dependence of (a) contact angle and (b) sliding angle on the X_{OH}, respectively. Insets are the shapes of a water droplet (4 μL) on the related surfaces.

In this work, the surface adhesion is our major interest. From Figure 3a, one can observe that when the X_{OH} is increased from 0 to 0.3, all the surfaces have similar superhydrophobicity with contact angles larger than 150°, whereas the dynamic properties are rather different (in this work, the superhydrophobic adhesion is our interest, thus the surface prepared with X_{OH} > 0.3 will not be considered in the following research for the loss of superhydrophobicity; for more discussion about the superhydrophobicity of the surfaces prepared with X_{OH} = 0–0.3, see the Supporting Information, Figure S5). On the surfaces prepared with X_{OH} = 0 and 0.1, a water droplet can roll with a low sliding angle less than 4° (Figure 3b). When the X_{OH} is increased to 0.2, the sliding angle increases to about 12°, further increasing the X_{OH} to 0.3, one can find that the water droplet would be pinned on the surface (inset in Figure 3b, the sliding angles 90° represents the water droplet is pinned on the surface; for more information, see the Supporting Information, Figure S6). In this work, the contact angle hysteresis (CAH) for the droplets on these surfaces were also investigated, and different dynamic performances of the droplets can be ascribed to different CAH.[74] As shown in Table 1, it can be seen that with an increase in the X_{OH}, the CAH increases. From the above, it can be concluded that by simply changing the X_{OH} of the modified solutions, the water mobility on the surfaces can be controlled.

Table 1. Advancing Contact Angles (θ_a), Receding Contact Angles (θ_r) and the CAH ($\Delta\theta = \theta_a - \theta_r$) for the Surfaces Modified with Different Solutions (X_{OH} = 0–0.3)

	X_{OH}			
	0	0.1	0.2	0.3
θ_a (deg)	159	158	155	153
θ_r (deg)	157	155	146	125
$\Delta\theta = \theta_a - \theta_r$ (deg)	2	3	9	28

Different dynamic performances mean the surfaces have different adhesions. Herein, the adhesive forces of the obtained surfaces were examined accurately by a high-sensitivity microelectromechanical balance system. As shown in Figure 4a–c, for the presence of adhesive force, the droplet has some distortion after contact with the surface (prepared with X_{OH} = 0.3). Figure 4d shows the force–distance curves for the superhydrophobic surfaces obtained with different X_{OH}. It can be observed that the maximum adhesive force for the as-prepared surfaces is different, and increases from about 8 μN to 65 μN as the X_{OH} is increased from 0 to 0.3 (Figure 4e).

To have a good understanding of the water-adhesion behavior on the as-prepared surfaces, we carefully analyzed the mechanism that influences the adhesive force. It is believed that the tunable effect of the adhesion can be explained as the following two reasons: one is the different number of hydrogen bonds for the variation of surface chemistry; the other is the variation of liquid/solid contact area because of the capillary effect that results from the combined effect of hydroxyl groups and microstructures on the substrate. When the substrate was modified with single $HS(CH_2)_9CH_3$ (X_{OH} = 0), all the molecules on the surface are hydrophobic and only water-repellent force is present (Figure 5b), the interaction between the surface and the water droplet is extremely weak and a layer of air can be trapped among the surface microstructures (Figure 5a). Therefore, a water droplet can roll with a low sliding angle on the surface (Figure 3b) and the surface shows a low adhesive force (Figure 4b). When the X_{OH} is increased, more hydroxyl groups would be assembled on the surface. As is known, hydroxyl group is a common hydrophilic group and can form hydrogen bond with the water molecules,[75] thus on the surface, in addition to the water-repellent force provided by the alkyl groups, a new water-adhesive force arises for the appearance of hydrogen bonds (Figure 5d), and such water-adhesive force increases as the X_{OH} is increased because more hydrogen bonds would be produced. In addition to the chemical factor, surface microstructures are also important for the surface adhesion because it would be helpful in the variation of the liquid/solid

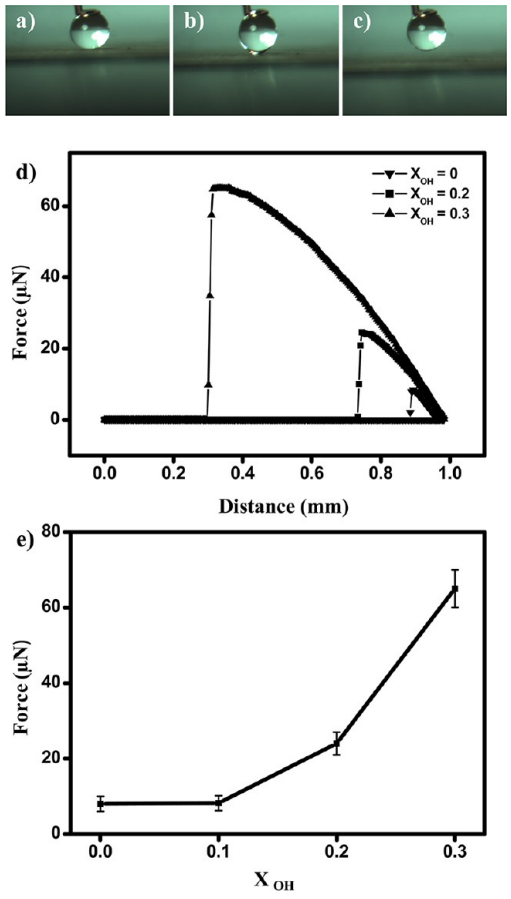

Figure 4. Dynamic adhesion measurement on the as-prepared surface: (a–c) CCD images for a typical measurement process. (d) Force–distance curves on the superhydrophobic surfaces prepared with X_{OH} = 0, 0.2, and 0.3, respectively. (e) Dependence of the adhesive force on the X_{OH}.

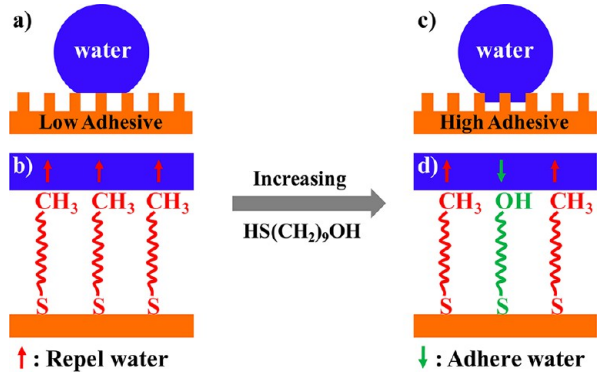

Figure 5. Schematic illustration of liquid/solid interactions: (b) when the surface is modified with single hydrophobic $HS(CH_2)_9CH_3$, (a) the water droplet resides in the low adhesive composited state with little liquid/solid contact area; (d) as the $HS(CH_2)_{11}OH$ is increased, the hydrogen bond between the water molecules and the hydroxyl groups would be formed; (c) meanwhile, the liquid/solid contact area can be increased because of the capillary effect results from the combined effect of hydrophilic hydroxyl groups and microstructures on the surface, thus increasing the surface adhesion.

contact area. In the case of surface modified with pure hydrophobic $HS(CH_2)_9CH_3$, the microstructure has a crucial role in decreasing the liquid/solid contact area for the presence of air among the microstructures (Figure 5a).[26] Whereas when the X_{OH} is increased and hydroxyl groups were introduced onto the surface, because the hydrophilic property of hydroxyl groups, water can enter into the microstructures on the surface for the capillary effect,[73,75] thus increasing the contact area between the surface and water droplet (Figure 5b), which can also be proved by the results derived from the Cassie equation

$$\cos\theta_c = f_1 \cos\theta - f_2 \quad (3)$$

where (θ_c) and (θ) and are the water contact angles of the hierarchical structured copper substrate and the flat copper substrate after assembling with mixed thiols, respectively, f_1 is the fraction of solid substrate in contact with water, and f_2 is the fraction of air in contact with water, (i.e., $f_1 + f_2 = 1$). In this work, θ are 100, 99, 96, and 94° for the surface modified with X_{OH} = 0, 0.1, 0.2, and 0.3, respectively (see the Supporting Information, Figure S5). Correspondingly, the θ_c on rough surfaces are 158, 157, 155, and 152° (Figure 3a), respectively. According to the above equation, the liquid/solid contact fraction for the surfaces prepared with X_{OH} = 0, 0.1, 0.2, and 0.3 are 0.088, 0.094, 0.106, and 0.125, respectively, indicating that the liquid/solid contact area increases as the X_{OH} is increased. Thus, the increase of the surface adhesion with increasing the X_{OH} is not only because of the appearance of hydrogen bonds, but also for the increased liquid/solid contact area. Therefore, as shown in Figure 4b, the adhesive force increases as X_{OH} is increased.

From the above explanation, it can be found that the amount of the hydroxyl groups on the surfaces is a crucial factor in this work to tune the surface adhesion. To further prove the effect of the hydroxyl groups on the surface adhesion, the surface prepared with X_{OH} = 0.3 was treated with trichloro(propyl)-silane (TLPS) to decrease the amount of hydroxyl groups on the surface. From the IR spectrum (see the Supporting Information, Figure S7), it is easy to find that compared with the original surface, a new broad peak at 970–1180 cm^{-1} assigned to the Si–O vibration appears after reacting with the TLPS, indicating that the propyl groups have been successfully grafted onto the surface *via* the reaction between the silane and the hydroxyl groups. This resulted in the decrease in hydroxyl group content. Then it would be reasonable to expect that the water-adhesive force should be weakened whereas the water-repellent force should be strengthened. The results of the dynamic wettability measurements show that after reaction with TLPS, the surface transformed from the high adhesive pinning stated to the low adhesive rolling state, and a water droplet can roll with a sliding angle lower than 5° on the surface (see the Supporting Information Figure S8). These results further demonstrate that hydrophilic hydroxyl groups contribute to water adhesion and the adjustment of the hydroxyl group amount can modulate the surface adhesion.

In addition to the tunable adhesion, the obtained surfaces exhibit a good acid/base-resisting property. As shown in Figure 6, as the water pH is changed between 2 and 12, the contact angles and the adhesive forces have no apparent variation within the errors. The surface has the similar contact angles and adhesive forces for acid/basic water droplets with that of the neutral water droplet, means that the surfaces have a particular chemical stability. Furthermore, the surfaces can retain such stability even after at least 2 months without special protection, indicating that the surface possesses good durability.

These special abilities allow the obtained surfaces to be used in a wide range of applications, for example, in the droplet-

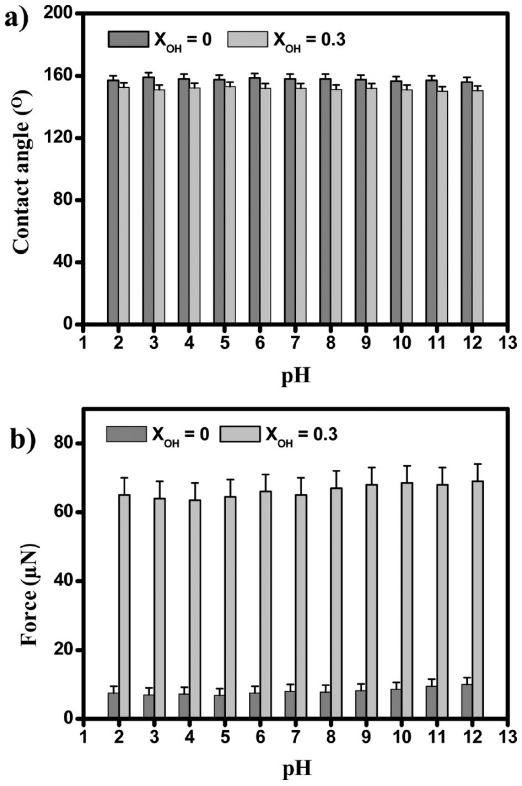

Figure 6. Statistics of the (a) contact angles and (b) adhesive forces for a water droplet with different pH values on the surfaces prepared with X_{OH} = 0 and 0.3, respectively.

based microreactors. Recently, such droplet-based microreactors especially the drop-to-drop settings have shown prominent advances in enzymatic kinetics protein crystallization, and some other biochemical reactions.[76−78] Herein, we demonstrate an application of the obtained superhydrophobic surfaces in the droplet-based microreactors for the detection of vitamin C. As shown in Figure 7, the obtained superhydrophobic surfaces with different adhesive forces were used as the reaction substrates, and a metal ring was used to transport the water droplets. A water droplet (5 μL) containing 2,6-dichloroindophenol sodium salt, which is suitable for the vitamin C detection and shows dark blue was first put on a low adhesive superhydrophobic surface, and then was carried by the metal ring (Figure 7a−d), subsequently, this droplet was used to contact with another water droplet containing the vitamin C depositing on a high adhesive superhydrophobic surface (Figure 7e, f). After contact, the two droplets coalesced and the color of the microdroplet disappeared for the reaction between 2,6-dichloroindophenol sodium salt and vitamin C (Figure 7g−i). At last, because of the high adhesion, the final droplet would be transferred from the metal ring to the surface (Figure 7j−l, see the Supporting Information, Figure S9). Thus a qualitative detection of vitamin C was completed assisted by our surfaces.

CONCLUSIONS

In conclusion, a facile approach was developed to fabricate superhydrophobic surfaces with controlled adhesion based on design of heterogeneous chemical composition on the hierarchical structured CuO substrate. By simply changing the concentration of $HS(CH_2)_{11}OH$ in the modified solution (containing both $HS(CH_2)_{11}OH$ and $HS(CH_2)_9CH_3$), tunable adhesive surfaces can be obtained and the adhesive force can be controlled between extremely low (~8 μN) and very high (~65 μN). The tunable effect can be explained as the following two reasons: one is the different number of hydrogen bond for the variation of surface chemistry; and the other is the variation of liquid/solid contact area because of the capillary effect that results from the combined effect of hydroxyl groups and microstructures on the substrate. Noticeably, the obtained surfaces have excellent chemical resistance to acid and alkali. At last, we provide a demonstration of application of our surfaces in the droplet-based microreactors for the detection of vitamin C. The results reported here would be useful for further understanding the influence of the surface chemistry on the surface adhesion, which is crucial for the design and preparation of surfaces with controlled adhesion. Meanwhile, because of the tunable adhesions, the obtained surfaces are potentially useful in many applications, such as microfluidic devices, no-loss water droplet transportation, and droplet-based biodetection.

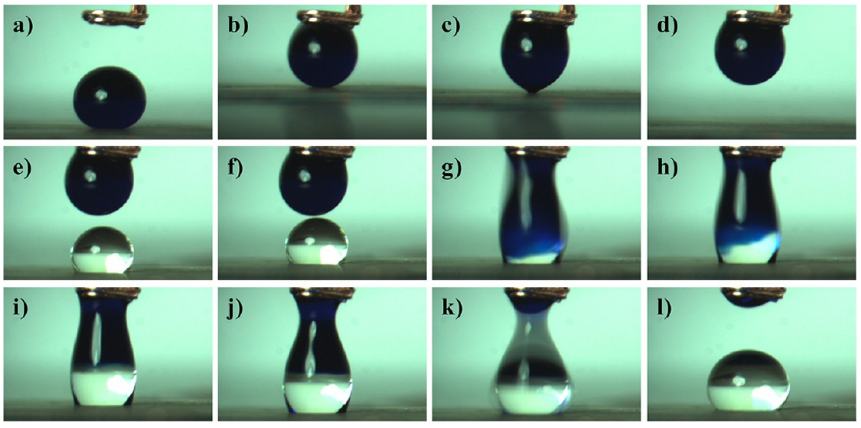

Figure 7. Applying the tunable adhesive superhydrophobic surfaces in the droplet-based microreactor. (a−d) Water droplet (5 μL) containing 2,6-dichloroindophenol sodium salt was transported from a low adhesive superhydrophobic surface to the metal cap. (e, f) Coalescence of the droplet to another droplet (5 μL) containing vitamin C on the high adhesive superhydrophobic surface. (g−i) After contact, the two droplets coalesced and the color disappeared for the reaction between 2,6-dichloroindophenol sodium salt and vitamin C. (j, l) The final droplet would be transferred from the metal ring to the high adhesive surface.

■ ASSOCIATED CONTENT

Supporting Information

SEM images of the copper surfaces after immersion in the NaOH and $(NH_4)_2S_2O_8$ solution for different times; SEM image of the nanowires on the substrate; shape of a water droplet on the as-prepared CuO surface; discussion of the superhydrophobicity on the rough substrates prepared with X_{OH} from 0 to 0.3; video record about the surface prepared with different X_{OH} before and after contact the droplet; IR results for the surfaces prepared with X_{OH} = 0.3 before and after reaction with TLPS; shapes of a water droplet on the surface prepared with X_{OH} = 0.3 before and after reaction with TLPS; detection of vitamin C with two low adhesive superhydrophobic surfaces. This material is available free of charge via the Internet at http://pubs.acs.org.

■ AUTHOR INFORMATION

Corresponding Author

*E-mail: keningsunhit@163.com. Tel: (+86) 045186412153. Fax: (+86) 045186412153.

Notes

The authors declare no competing financial interest.

■ ACKNOWLEDGMENTS

This work is supported by the Open Project of State Key Laboratory of Urban Water Resource and Environment, Harbin Institute of Technology (ES201008); Project HIT. NSRIF. 2009087 supported by Natural Scientific Research Innovation Foundation in Harbin Institute of Technology. The Research Fund for the Doctoral Program of Higher Education of china (20112302120062). China Postdoctoral Science Foundation (2011M500650).

■ REFERENCES

(1) Yao, X.; Song, Y. L.; Jiang, L. *Adv. Mater.* **2011**, *23*, 719−734.
(2) Lafuma, A.; Quéré, D. *Nat. Mater.* **2003**, *2*, 457−460.
(3) Blossey, R. *Nat. Mater.* **2003**, *2*, 301−306.
(4) Roach, P.; Shirtcliffe, N. J.; Newton, M. I. *Soft Matter.* **2008**, *4*, 224−240.
(5) Zhang, X.; Shi, F.; Niu, J.; Jiang, Y.; Wang, Z. *J. Mater. Chem.* **2008**, *18*, 621−633.
(6) Li, X. M.; Reinhoudt, D.; Crego-Calama, M. *Chem. Soc. Rev.* **2007**, *36*, 1350−1368.
(7) Xiu, Y.; Zhu, L.; Hess, D. W.; Wong, C. P. *Nano Lett.* **2007**, *7*, 3388−3393.
(8) Zhang, Y.; Chen, Y.; Shi, L.; Li, J.; Guo, Z. *J. Mater. Chem.* **2012**, *22*, 799−815.
(9) Liu, X.; Liang, Y.; Zhou, F.; Liu, W. *Soft Matter.* **2012**, *8*, 2070−2086.
(10) Xue, Z.; Wang, S.; Lin, L.; Chen, L.; Liu, M.; Feng, L.; Jiang, L. *Adv. Mater.* **2011**, *23*, 4270−4273.
(11) Yuan, J. K.; Liu, X. G.; Akbulut, O.; Hu, J. Q.; Suib, S. L.; Kong, J.; Stellacci, F. *Nat. Nanotechnol.* **2008**, *3*, 332−336.
(12) Jin, M.; Wang, J.; Yao, X.; Liao, M.; Zhao, Y.; Jiang, L. *Adv. Mater.* **2011**, *23*, 2861−2864.
(13) Zhang, J.; Seeger, S. *Adv. Funct. Mater.* **2011**, *21*, 4699−4704.
(14) Min, W. L.; Jiang, B.; Jiang, P. *Adv. Mater.* **2008**, *20*, 3914−3918.
(15) Sheparovych, R.; Motornov, M.; Minko, S. *Adv. Mater.* **2009**, *21*, 1840−1844.
(16) Cottin-Bizonne, C.; Barrat, J. L.; Bocquet, L.; Charlaix, E. *Nat. Mater.* **2003**, *2*, 237−240.
(17) Jin, M. H.; Feng, X. J.; Feng, L.; Sun, T. L.; Zhai, J.; Li, T. J.; Jiang, L. *Adv. Mater.* **2005**, *1*, 1977−1981.
(18) Hong, X.; Gao, X. F.; Jiang, L. *J. Am. Chem. Soc.* **2007**, *129*, 1478−1479.
(19) Liu, M.; Zheng, Y.; Zhai, J.; Jiang, L. *Acc. Chem. Res.* **2010**, *43*, 368−377.
(20) Barthlott, W.; Neinhuis, C. *Planta* **1997**, *202*, 1−8.
(21) Feng, L.; Li, S.; Li, Y.; Zhang, L.; Zhai, J.; Song, Y.; Liu, B.; Jiang, L.; Zhu, D. *Adv. Mater.* **2002**, *14*, 1857−1860.
(22) Chen, P.; Chen, L.; Han, D.; Zhai, J.; Zheng, Y.; Jiang, L. *Small* **2009**, *5*, 908−912.
(23) Gao, X. F.; Jiang, L. *Nature* **2004**, *432*, 36−36.
(24) Hu, D. L.; Chan, B.; Bush, J. W. M. *Nature* **2003**, *424*, 663−666.
(25) Bhushan, B.; Her, E. K. *Langmuir* **2010**, *26*, 8207−8217.
(26) Feng, L.; Zhang, Y.; Xi, J.; Zhu, Y.; Wang, N.; Xia, F.; Jiang, L. *Langmuir* **2008**, *24*, 4114−4119.
(27) Autumn, K.; Sitti, M.; Liang, Y. C. A.; Peattie, A. M.; Hansen, W. R.; Sponberg, S.; Kenny, T. W.; Fearing, R.; Israelachvili, J. N.; Full, R. J. *Proc. Natl. Acad. Sci. U.S.A.* **2002**, *99*, 12252−12256.
(28) Liu, K.; Du, J.; Wua, J.; Jiang, L. *Nanoscale* **2012**, *4*, 768−772.
(29) Xia, F.; Jiang, L. *Adv. Mater.* **2008**, *20*, 2842−2858.
(30) Uchida, K.; Nishikawa, N.; Izumi, N.; Yamazoe, S.; Mayama, H.; Kojima, Y.; Yokojima, S.; Nakamura, S.; Tsujii, K.; Irie, M. *Angew. Chem., Int. Ed.* **2010**, *49*, 5942−5944.
(31) Cheng, Z.; Du, M.; Lai, H.; Zhang, N.; Sun, K. *Nanoscale* **2013**, *5*, 2776−2783.
(32) Huang, X.; Kim, D.; Im, M.; Lee, J.; Yoon, J.; Choi, Y. *Small* **2009**, *5*, 90−94.
(33) Zhao, Y.; Lu, Q. H.; Chen, D. S.; Wei, Y. *J. Mater. Chem.* **2006**, *16*, 4504−4509.
(34) Lai, Y.; Gao, X.; Zhuang, H.; Huang, J.; Lin, C.; Jiang, L. *Adv. Mater.* **2009**, *21*, 3799−3803.
(35) Zhao, X. D.; Fan, H. M.; Liu, X. Y.; Pan, H.; Xu, H. Y. *Langmuir* **2011**, *27*, 3224−3228.
(36) Cheng, Z.; Gao, J.; Jiang, L. *Langmuir* **2010**, *26*, 8233−8238.
(37) Zhang, D.; Chen, F.; Yang, Q.; Yong, J.; Bian, H.; Ou, Y.; Si, J.; Meng, X.; Hou, X. *ACS Appl. Mater. Interfaces* **2012**, *4*, 4905−4912.
(38) Shahsavan, H.; Arunbabu, D.; Zhao, B. *Macromol. Mater. Eng.* **2012**, *297*, 743−760.
(39) Zhu, S.; Li, Y.; Zhang, J.; Lü, C.; Dai, X.; Jia, F.; Gao, H.; Yang, B. *J. Colloid Interface Sci.* **2010**, *344*, 541−546.
(40) Yong, J.; Chen, F.; Yang, Q.; Zhang, D.; Bian, H.; Du, G.; Si, J.; Meng, X.; Hou, X. *Langmuir* **2013**, *29*, 3274−3279.
(41) Pu, J.; Wan, S.; Lu, Z.; Zhang, G.; Wang, L.; Zhang, X.; Xue, Q. *J. Mater. Chem. A* **2013**, *1*, 1254−1260.
(42) Wu, D.; Wu, S.; Chen, Q.; Zhang, Y.; Yao, J.; Yao, X.; Niu, L.; Wang, J.; Jiang, L.; Sun, H. *Adv. Mater.* **2011**, *23*, 545−549.
(43) Zhao, W.; Wang, L.; Xue, Q. *J. Phys. Chem. C* **2010**, *114*, 11509−11514.
(44) Li, J.; Liu, X.; Ye, Y.; Zhou, H.; Chen, J. *J. Phys. Chem. C* **2011**, *115*, 4726−4729.
(45) Bhushan, B.; Her, E. K. *Langmuir* **2010**, *26*, 8207−8217.
(46) Yang, Z.; Chien, F.; Kuo, C.; Chueh, D.; Chen, P. *Nanoscale* **2013**, *5*, 1018−1025.
(47) Dawood, M. K.; Zheng, H.; Liew, T. H. *Langmuir* **2011**, *27*, 4126−4133.
(48) Cha, T.; Yi, J. W.; Moon, M.; Lee, K.; Kim, H. *Langmuir* **2010**, *26*, 8319.
(49) Teisala, H.; Tuominen, M.; Aromaa, M.; Stepien, M.; Mäkelä, J. M.; Saarinen, J. J.; Toivakka, M.; Kuusipalo, J. *Langmuir* **2012**, *28*, 3138−8326.
(50) Wolfs, M.; Darmanin, T.; Guittard, F. *Soft Matter* **2012**, *8*, 9110−9114.
(51) Ou, J.; Hu, W.; Li, C.; Wang, Y.; Xue, M.; Wang, F.; Li, W. *ACS Appl. Mater. Interfaces* **2012**, *4*, 5737−5741.
(52) Pisuchpen, T.; Chaim-ngoen, N.; Intasanta, N.; Supaphol, P.; Hoven, V. P. *Langmuir* **2011**, *27*, 3654−3661.
(53) Wang, C.; Wang, T.; Liao, C.; Kuo, S.; Lin, H. *J. Phys. Chem. C* **2011**, *115*, 16495−16500.
(54) Darmanin, T.; Guittard, F. *Soft Matter* **2013**, *9*, 1500−1505.
(55) Guo, Z.; Chen, X.; Li, J.; Liu, J.; Huang, X. *Langmuir* **2011**, *27*, 6193−6200.

(56) Ramakrishna, S. N.; Clasohm, L. Y.; Rao, A.; Spencer, N. D. *Langmuir* **2011**, *27*, 9972−9978.
(57) Perry, G.; Coffinier, Y.; Thomy, V.; Boukherroub, R. *Langmuir* **2012**, *28*, 389−395.
(58) Bhushan, B. *Langmuir* **2012**, *28*, 1698−1714.
(59) Jeong, C.; Choi, C. *ACS Appl. Mater. Interfaces* **2012**, *4*, 842−848.
(60) Lee, W.; Park, B. G.; Kim, D. H.; Ahn, D. J.; Park, Y.; Lee, S. H.; Lee, K. B. *Langmuir* **2010**, *26*, 1412−1415.
(61) Balu, B.; Breedveld, V.; Hess, D. W. *Langmuir* **2008**, *24*, 4785−4790.
(62) Ishii, D.; Yabu, H.; Shimomura, M. *Chem. Mater.* **2009**, *21*, 1799−1801.
(63) Zhao, N.; Xie, Q.; Kuang, X.; Wang, S.; Li, Y.; Lu, X.; Tan, S.; Shen, J.; Zhang, X.; Zhang, Y.; Xu, J.; Han, C. C. *Adv. Funct. Mater.* **2007**, *17*, 2739−2745.
(64) Lai, Y.; Lin, C. J.; Huang, J. Y.; Zhuang, H. F.; Sun, L.; Nguyen, T. *Langmuir* **2008**, *24*, 3867−3873.
(65) Wang, M.; Chen, C.; Maab, J.; Xu, J. *J. Mater. Chem.* **2011**, *21*, 6962−6967.
(66) Zhu, X.; Zhang, Z.; Men, X.; Yang, J.; Xu, X. *ACS Appl. Mater. Interfaces* **2010**, *2*, 3636−3641.
(67) Chen, X.; Kong, L.; Dong, D.; Yang, G.; Yu, L.; Chen, J.; Zhang, P. *J. Phys. Chem. C* **2009**, *113*, 5396−5401.
(68) Bertilsson, L.; Liedberg, B. *Langmuir* **1993**, *9*, 141−149.
(69) Ulman, A. *Chem. Rev.* **1996**, *96*, 1533−1554.
(70) Yu, Y.; Wang, Z.; Jiang, Y.; Shi, F.; Zhang, X. *Adv. Mater.* **2005**, *17*, 1289−1293.
(71) Feng, X.; Jiang, L. *Adv. Mater.* **2006**, *18*, 3063−3078.
(72) Cassie, A. B. D.; Baxter, S. *Trans. Faraday Soc.* **1944**, *40*, 546−551.
(73) Wenzel, R. N. *Ind. Eng. Chem.* **1936**, *28*, 988−994.
(74) Yüce, M. Y.; Demirel, A. L.; Menzel, F. *Langmuir* **2005**, *21*, 5073−5078.
(75) Wang, D.; Liu, Y.; Liu, X.; Zhou, F.; Liua, W.; Xue, Q. *Chem. Commun.* **2009**, 7018−7020.
(76) Song, H.; Chen, D. L.; Ismagilov, R. F. *Angew. Chem., Int. Ed.* **2006**, *45*, 7336−7356.
(77) deMello, A. J. *Nature* **2006**, *442*, 394−402.
(78) Su, B.; Wang, S. T.; Song, Y. L.; Jiang, L. *Soft Matter* **2012**, *8*, 631−635.